**Review**

Published in *Analytical and Bioanalytical Chemistry* **384** (2006) 1071–1086.
**Received:** 11 March 2005 ~ **Revised:** 28 April 2005 ~ **Accepted:** 29 April 2005 ~ **Published online:** 7 June 2005
doi: 10.1007/s00216-005-3281-6


# Photoacoustic spectroscopy for process analysis

**Thomas Schmid**

Institute of Hydrochemistry, Technische Universität München, Marchioninistr. 17, 81377 Munich, Germany

**Email:** thomas@schmid.eu.com
**Phone:** +49-89-218078240
**Fax:** +49-89-218078255

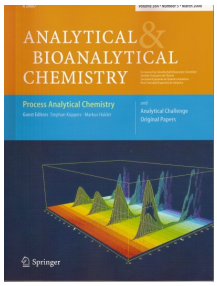


**Abstract** *Photoacoustic spectroscopy (PAS) is based on the absorption of electromagnetic radiation by analyte molecules. The absorbed energy is measured by detecting pressure fluctuations in the form of sound waves or shock pulses. In contrast to conventional absorption spectroscopy (such as UV/Vis spectroscopy), PAS allows the determination of absorption coefficients over several orders of magnitude, even in opaque and strongly scattering samples. Small absorption coefficients, such as those encountered during trace gas monitoring, can be detected with cells with relatively short pathlengths. Furthermore, PA techniques allow absorption spectra of solid samples (including powders, chips or large objects) to be determined, and they permit depth profiling of layered systems. These features mean that PAS can be used for on-line monitoring in technical processes without the need for sample preparation and to perform depth-resolved characterization of industrial products. This article gives an overview on PA excitation and detection schemes employed in analytical chemistry, and reviews applications of PAS in process analytical technology and characterization of industrial products.*

**Keywords** Photoacoustic spectroscopy (PAS) – Process analysis – Industrial materials – On-line monitoring – Non-destructive testing

# 1 Introduction

Photoacoustic spectroscopy (PAS) is based on the absorption of electromagnetic radiation by analyte molecules. Non-radiative relaxation processes (such as collisions with other molecules) lead to local warming of the sample matrix. Pressure fluctuations are then generated by thermal expansion, which can be detected in the form of acoustic or ultrasonic waves (see Fig. 1).

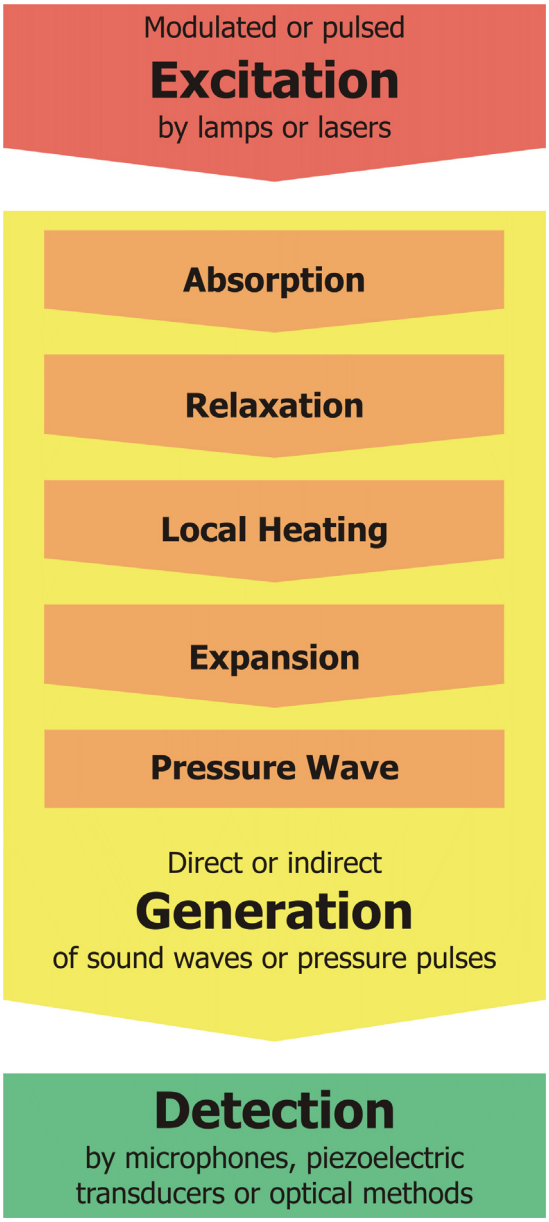


**Fig. 1** Principle of excitation, signal generation and detection in a photoacoustic experiment.

The photoacoustic effect was discovered by A.G. Bell in 1880. He found that thin discs emit sound when exposed to a rapidly interrupted beam of sunlight [1, 2]. By placing different absorbing substances in contact with the ear using a hearing tube, he was able to detect absorption in both the visible and the invisible regions of the solar spectrum. This spectrophone was used in his experiments on wireless transmission of sound. After additional experiments by Tyndall [3] and Röntgen [4], and some initial analytical applications in the 1930s and 1940s [5, 6], interest in the photoacoustic effect declined over the following decades.

The first applications of the effect to trace gas monitoring were reported in the late 1960s and early 1970s [7–9]. Important steps leading to this rediscovery of the effect for analytical purposes were the invention of the laser as an intense light source, the development of highly sensitive sound detectors (such as condenser microphones and piezoelectric transducers), and the first comprehensive theoretical description of the photoacoustic effect in solids by Rosencwaig and Gersho: the so-called RG theory [10].

This article gives an overview on PA excitation and detection schemes currently employed in analytical chemistry, and reviews applications of PAS in process analysis (see Table 1) and the characterization of industrial products.

# 2 PAS features

Conventional absorption spectroscopy is based on excitation by electromagnetic radiation with intensity $I_0$ and the measurement of reflected or transmitted light intensity $I$. Thus, the absorbance is derived indirectly from transmittance or reflectance, whereas in PAS pressure waves are detected which are generated directly by the absorbed energy. Conventional transmission spectroscopy is often hampered by low absorption coefficients ($I \approx I_0$), the opacity of the sample ($I \approx 0$) and scattering particles. In these cases, the use of PAS is advantageous.

One of the main advantages of PAS is its wide dynamic range, allowing the determination of absorption coefficients over several orders of magnitude. This analytical technique can be applied to the measurement of weak absorption using PA cells with relatively small pathlengths, allowing compact and mobile set-ups. On the other hand, dilution is not necessary in most cases

when highly absorbing and opaque samples are investigated by PAS. It is even possible to determine absorption spectra for opaque solids.
In conventional absorption spectroscopy the signal is influenced by both light absorption and scattering. Since scattering does not change the thermal state of the sample, PA signals are generated only by the absorbed fraction of the excitation beam. Thus, filtering the sample to remove scattering particles is not usually necessary. Similar to fluorescence spectroscopy, the signal from a photoacoustic experiment depends on the incident radiation power. Thus, the sensitivity can be tuned to the desired range by choosing an appropriate radiation source (for example, a lamp versus a laser). Another advantage of PAS is the possibility of depth-resolved investigation of solid samples. These features are beneficial if on-line monitoring of technical processes without sample preparation is required, or the depth-resolved characterization of industrial products.

# 3 PAS techniques

In this section, various schemes for the excitation, generation, and detection of PA signals are presented. Although, many combinations of these schemes are possible, this communication focuses on the most common techniques, which are summarized in Fig. 2.

## 3.1 Excitation

As mentioned above, the PA effect is based on the sample heating produced by optical absorption. In order to generate acoustic waves, which can be detected by pressure sensitive transducers, periodic heating and cooling of the sample is necessary to generate pressure fluctuations. In principle, there are two ways to realize PA pressure fluctuations: modulated and pulsed excitation [11–13].

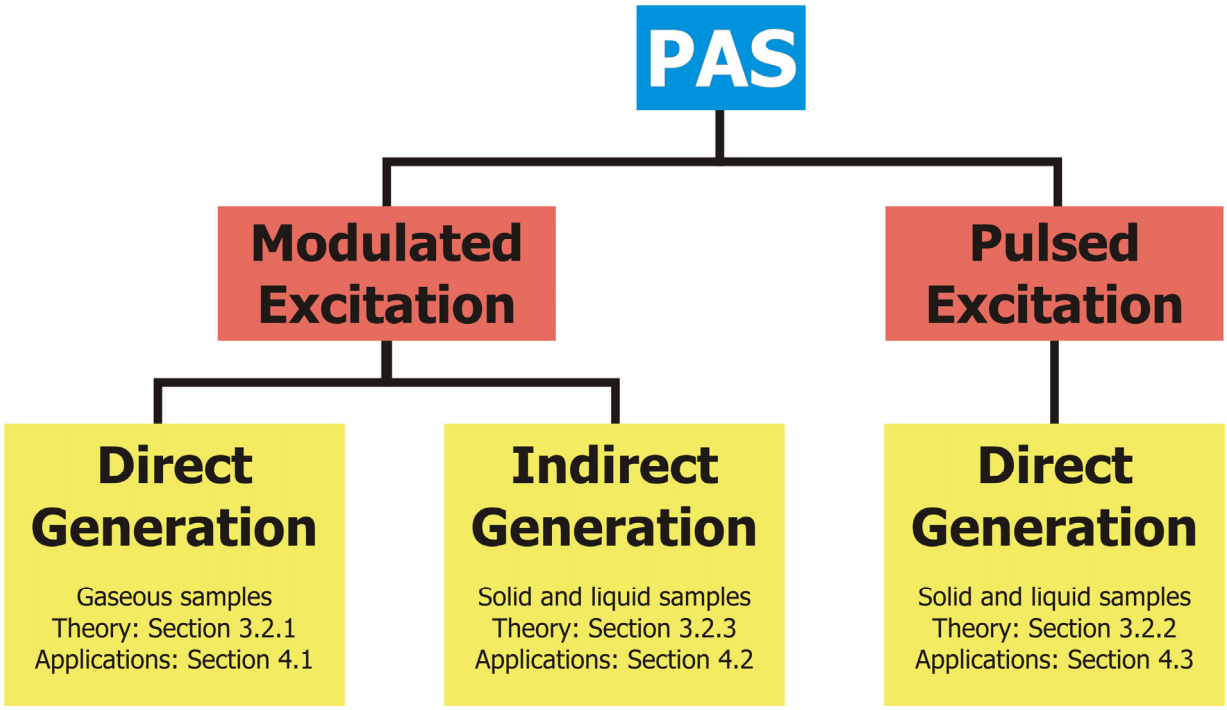


**Fig. 2** Most common combinations of excitation and signal generation in photoacoustic spectroscopy.

**Table 1: Applications of PAS to process analysis described in this article.**

| Section | Application | Analyte or measurand | Ref. |
|---|---|---|---|
| **4.1 Gas phase analysis** | Monitoring of workplaces and clean rooms | $NH_3$ | [95-97] |
| | | Solvent vapors | [100] |
| | Monitoring of automobile and industrial exhaust gases | $NO_2$ | [98] |
| | | $CH_4$ | [99] |
| | | Multicomponent analysis: $NO_X$, water vapor, $CO_2$, carbohydrates | [102-105] |
| | | Soot particles | [106-108] |
| | Fire detection and prevention | Combustion and flammable gases | [101] |
| | Gas monitoring during postharvest processing and storage of fruits | Ethylene | [109, 110] |
| | | Multicomponent analysis: $NH_3$, $O_3$, ethylene, alcohols | [111, 112] |
| | Other agricultural applications | Gas emissions from extensively managed grassland and fields, seeds, and animal husbandry | [113-118] |
| | Monitoring of food packaging | Water vapor | [119] |
| | Indirect sampling of condensed matter | Total inorganic carbonate (TIC) in liquid and solid samples | [120] |
| | | Pentachlorophenol (PCP) in treated wood samples | [121] |

| | | | |
|---|---|---|---|
| **4.2 Indirect PA generation in condensed matter** | Characterization of semiconductors | Band gap | [122-124] |
| | | Thermal diffusivity | [125] |
| | Characterization of paper materials and coatings | Thickness and moisture content of varnish layers (UV/Vis-PAS) | [128] |
| | | Depth profiles of biodegradable paper coatings (FTIR-PAS) | [138] |
| | Polymer research | IR absorption spectra of polymers (e.g. in form of powders, chips or membranes) | [132, 133] |
| | | Thermal diffusivity | [130, 131] |
| | | Depth profiles | [134-137] |
| | Characterization of fossil fuels | Hydrocarbons in coaking coal | [139] |
| | | Hydrocarbons in different distillation fractions | [140, 141] |
| **4.3 Direct PA generation in condensed matter** | Monitoring of contaminants in water | Crude oil, hydrocarbons | [146-148] |
| | Monitoring of textile dyeing processes | Textile dyes | [149-151] |
| | Monitoring of biofilms and investigation of biocide efficacy | Biomass, thickness, depth profiles | [152-154] |
| | Applications of optical detection methods in PAS | Mechanical properties of paper materials | [155] |
| | | Painting thickness | [156] |
| | | Viscoelastic properties, thermal diffusivity and thickness of thin films | [157] |

### 3.1.1 Modulated excitation

In modulated excitation schemes, radiation sources are employed whose intensity fluctuates periodically in the form of a square or a sine wave, resulting in a 50% duty cycle. This can be realized for example by the mechanical chopping of a light source. A way to overcome the 50% duty cycle is to modulate the phase instead of the amplitude of the emitted radiation. Whereas chopped or modulated lamps or IR sources from commercial spectrometers are used for the determination of UV/Vis or IR absorption spectra of opaque solids, modulated continuous wave (cw) lasers are the most common sources for PA gas phase analysis. The modulation frequencies usually range from a few Hz up to several kHz. The resulting pressure fluctuations generate sound waves in the audible range, which can be detected by microphones in the gas phase. Data analysis is performed in the frequency domain. Therefore, lock-in amplifiers are used for signal recording, which allows the analysis of both the amplitude and the phase of the sound wave. Since the acoustic propagation during the relatively long illumination period is much larger than the dimensions of the sample in most cases, boundary conditions have to be taken into account. This means that eigenmodes of the PA cell play an important role. This fact can be utilized for signal enhancement by acoustic resonance. Thus, acoustic resonance curves must be considered in PA cell design. In solid samples, tuning of the modulation frequency allows depth-resolved investigations (see Sect. 3.2.3).

### 3.1.2 Pulsed excitation

In pulsed PAS, laser pulses with durations in the nanosecond range are usually employed for excitation. Since the repetition rates are in the range of a few Hz, the result is a short illumination followed by a much longer dark period: a low duty cycle. This leads to a fast and adiabatic thermal expansion of the sample medium resulting in a short shock pulse. Data analysis in this case is performed in the time domain. Therefore, the signal is recorded by oscilloscopes, boxcar systems, or fast A/D converters. Transformation of the signal pulse into the frequency domain results in a wide spectrum of acoustic frequencies up to the ultrasonic range. Thus, laser beams modulated in the form of a sine wave excite one single acoustic frequency, whereas short laser pulses are broadband acoustic sources. In solid samples, analysis of the time delay between laser pulse and pressure detection allows depth profiling, as explained in Sect. 3.2.2.

## 3.2 Signal generation

Induction of an acoustic wave by modulated or pulsed irradiation inside a gaseous, liquid or solid sample is termed direct PA generation. Here, detection takes place inside or at an interface of the sample (see Sects. 3.2.1 and 3.2.2). In indirect PA generation, heat is generated by modulated illumination inside a solid or liquid sample and transported to an interface. Subsequently, sound waves are generated and detected in the gas phase adjacent to the sample (see Sect. 3.2.3) [13].

### 3.2.1 Direct PA generation in gases

Chopped cw lasers or modulated laser diodes are employed for the modulated excitation of PA signals in gases. The modulated laser beam irradiates the gaseous sample inside a (usually cylindrical) PA cell, and sound waves with an acoustic frequency defined by the modulation frequency of the laser can be detected using microphones [14–16]. The signal amplitude can be described by

$$p = F W_0 \mu_a \quad (1)$$

where $W_0$ is the incident radiation power and a is the absorption coefficient of the sample. The proportionality factor $F$ is termed the cell constant. Figure 3 depicts the principal set-up of a PA cell for gas phase analysis.

In the so-called non-resonant mode, the modulation frequency is much lower than the first acoustic resonance frequency of the PA cell. In this case, the wavelength of the generated acoustic wave is larger than the cell dimensions. Thus, the generation of standing acoustic waves is not possible.

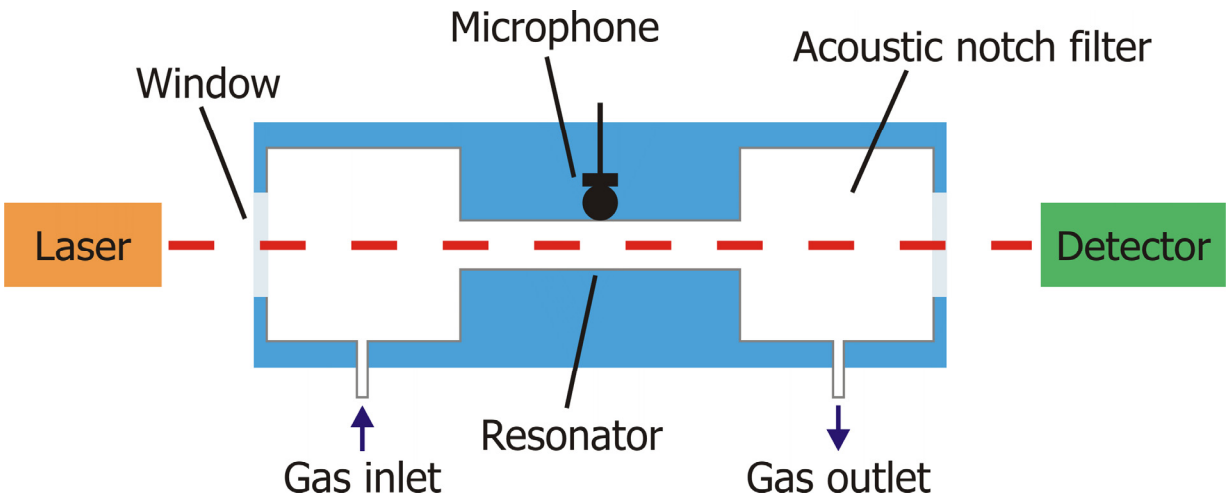


**Fig. 3** Set-up of a photoacoustic cell for gas phase analysis.

The cell constant $F$ is [17, 18]

$$F = \frac{G(\gamma - 1)L}{\omega V} \tag{2}$$

Here, $G$ is a geometric factor of the order of one, $\gamma$ is the adiabatic coefficient of the gas, $L$ and $V$ are the length and the volume of the cell, and $\omega = 2\pi\nu$ the modulation frequency. The PA signal is indirectly proportional to the modulation frequency and the cross-section $V/L$ of the cell. Thus, the signal increases with decreasing cell dimensions and modulation frequency. As the noise increases with a decrease in these parameters, there is a maximum in the $S/N$ ratio for a certain combination of cell size and modulation frequency [19].

With increasing modulation frequency, at a certain point the acoustic wavelength reaches the cell dimensions, and the resonant eigenmodes of the cell can be excited, leading to an amplification of the signal [20–23]. Resonance properties mainly depend upon the geometry and size of the cavity. The modulation frequency is tuned to one of the eigenfrequencies of the cell and thus the signal is amplified by a quality factor $Q_i$ resulting in a cell constant $F_{res}$ of [18, 19]:

$$F_{res} = Q_i \frac{C_i(\gamma - 1)}{\omega_i V} \tag{3}$$

where $C_i$ denotes a factor that depends on the positions of the laser beam and the microphone relative to the pressure distribution in the cell. The index $i$ indicates that $Q$ and $C$ are parameters describing the $i$th eigenmode of the cell. The quality factor can be described as the ratio between the accumulated energy in the resonator and the energy loss per cycle [17]. Signal amplification by the $Q$-factor can reach $10^3$. In resonant cells with high quality factors, the resonance profile becomes narrow and small drifts of modulation frequency or speed of sound in the gas mixture cause strong changes in $Q$. Therefore, moderate $Q$-factors are preferred in many applications [19, 20].

As mentioned in Sect. 3.1.2, pulsed excitation leads to broadband generation of various acoustic frequencies. Thus, in gas phase analysis by pulsed laser PAS, all eigenmodes of the cell can be excited simultaneously. The cell design is usually optimized to the excitation of one selected eigenmode, which is well separated from the neighboring ones. In this case, each laser pulse generates an exponentially decaying sine wave whose amplitude can be described by [19]:

$$p = \frac{C(\gamma - 1)}{V} E_0 \mu_a \tag{4}$$

Here, $E_0$ is the laser pulse energy. Note that the PA signal amplitude does not depend on $Q$-factor, modulation frequency or repetition rate. Thus, the signal does not depend on the speed of sound in the cell. In this case, the cell constant depends only

on the geometrical properties of the PA cell. If the signal is dominated by one eigenmode and the contributions of other eigenmodes can be neglected, cell constants can be calculated that are in good agreement with experimental results. Pulsed laser PAS can therefore be applied to absolute absorption measurements in gases [24].

### 3.2.2 Direct PA generation in liquids and solids

In condensed matter, short laser pulses are used for direct PA generation. The short illumination with relatively high peak power leads to an instantaneous adiabatic expansion of the medium, generating pressure pulses that propagate through the sample at the speed of sound. These ultrasonic pulses can be detected directly at a boundary of the sample by piezoelectric transducers or optical methods (see Sect. 3.3) [25]. As in other PA techniques, the signal amplitude depends linearly on the excitation energy and the absorption coefficient of the sample, and they can be described by [13, 26–28]:

$$p \propto \frac{\beta c^2}{C_p} E_0 \mu_a \tag{5}$$

where $\beta$, $c$ and $C_p$ denote the sample's thermal expansion coefficient, speed of sound, and heat capacity, respectively. If the signal in pulsed PAS is recorded time-resolved, the time delay $t$ between laser pulse and pressure detection can be determined, which represents the propagation time of the ultrasonic pulse through the sample. Thus, the depth $z$ of an absorbing object inside the sample can be calculated simply as follows [26–28]:

$$z = c\,t \tag{6}$$

Equation 6 corresponds to the principle of ultrasonic tomography. It should be pointed out that in ultrasonic tomography, reflections of pressure waves at acoustic impedance mismatches are detected. Thus, for a signal to occur in ultrasonic tomography, a change of the acoustic impedance $Z$ at an interface is needed, which is defined as

$$Z = \rho c \tag{7}$$

where is the density of the sample. In contrast to ultrasonic tomography, PA depth profiling allows the depth resolved detection of changes in optical absorption [26–35]. The maximum depth that can be investigated by pulsed PAS is limited by the optical penetration depth, $\delta = 1/\mu_a$. Since the decay length of acoustic waves is much higher than the optical penetration depth in many solid samples, beyond this limit depth profiling is possible by detecting laser-induced pressure pulses, which are reflected at acoustic impedance mismatches. This technique, which is similar to ultrasonic tomography, can be applied to the non-destructive testing of opaque solid materials, and is termed laser-induced ultrasound (LIU) [36–38]. Depth resolution of both pulsed PAS and LIU depends mainly on the time resolution of the ultrasonic detector. Corresponding to Eq. 6, the depth resolution can be calculated as the product of the temporal resolution of the detector and the speed of sound in the sample. If fast piezoelectric detectors and data recording with temporal resolutions in the nanosecond range are used, depth resolutions in the lower micrometer range can be realized. The maximum sampling depth can reach a few centimeters in weak absorbing and scattering samples. If piezoelectric detector arrays, scanning PA sensors, or suitable optical methods for detection are employed (see Sect. 3.3), two-dimensional and three dimensional imaging is feasible by pulsed PAS [39–44].

### 3.2.3 Indirect PA generation

Analysis of condensed matter by modulated PA excitation and subsequent detection of the directly generated acoustic wave by a microphone is not suitable due to strong acoustic impedance mismatches between solid and gas phase (see Sect. 3.3). Thus, an indirect scheme for PA generation is employed. Modulated warming of the sample is induced by modulated excitation. Subsequently, the heat deposited in the sample is transported to the interface of the sample with the adjacent gas phase [11–13]. This heat transport can be described as thermal wave. Thermal waves decay to 37% (1/e) of their initial intensity after propagating the thermal diffusion length $L$ [10, 45]:

$$L = \sqrt{\frac{D}{\pi \nu}} \tag{8}$$

Here, $D$ and are the thermal diffusivity of the sample and the modulation frequency of the excitation beam. After reaching the phase boundary, part of the thermal wave is transmitted into the adjacent gas phase. The resulting thermal expansion of the gas – usually inside a PA cell – leads to the generation of an acoustic wave, which can be detected by a microphone (see Fig. 4). As in other PA generation schemes, the amplitude of the sound wave increases with the absorption coefficient of the sample and the incident radiation power. The phase shift between modulated excitation and PA signal depends on the thermal diffusion time during signal generation. Thus, phase-dependent measurements allow depth-resolved investigations. The maximum phase angle that can be measured is one cycle, $2\pi$, resulting in a maximum depth of $2\pi L$. Since the signal amplitude is usually evaluated in PA measurements, depth-resolved measurements are performed by tuning the modulation frequency and influencing the thermal diffusion length. The higher the modulation frequency, the lower the thickness of the layer, which is represented by the PA signal. In indirect PA generation, the depth resolution is usually in the 100 nm range and the maximum sampling depth reaches a few hundred microns [45].

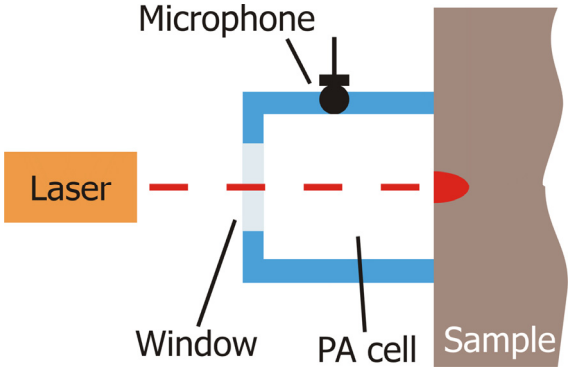


**Fig. 4** Indirect generation of photoacoustic waves for the analysis of solid and liquid samples.

For indirect generation and detection of PA signals, PA cells can be coupled to conventional spectrometers, allowing UV/Vis or IR absorption spectroscopy of opaque solid samples. A relatively common set-up for this purpose is FT-IR–PAS [45–47]. In this case, a Fourier transform IR spectrometer is used for excitation and PA signals are detected in a PA cell, which is in contact with the sample. In continuous scan FT-IR (CSFT-IR), the modulation frequency can be tuned by changing the interferometer moving mirror velocity. In step scan mode ($S^2$FT-IR), the excitation beam is modulated mechanically by a chopper for intensity modulation or by jittering the position of one of the interferometer mirrors, resulting in phase modulation [48].

## 3.3 Signal detection

Sound waves generated directly or indirectly in the gas phase are detected usually by condenser or electret microphones [11–13]. Detection of sound waves by microphones in condensed matter is typically not suitable. Due to high acoustic impedance mismatches, less than $10^{-4}$ of the acoustic energy is transferred from a solid sample to the adjacent gas phase [13]. In pulsed excitation of condensed matter, the application of microphones is additionally hampered due to their restricted bandwidth. Therefore, piezoelectric transducers are employed in many cases for the detection of ultrasonic pulses in liquid and solid samples [49, 50]. Quartz crystals, piezoelectric ceramics such as lead zirconate titanate (PZT) [51], lead metaniobate, and lithium niobate [52] as well as piezoelectric polymer films can be applied to the detection of laser-induced shock pulses [13]. The most common piezoelectric polymer is polyvinylidene fluoride (PVDF), which is available in different thicknesses ranging from 5 to 100 µm as a transparent film or coated with metals for electrical contact [53]. As the sensitivity of piezoelectric detectors usually increases with their thickness, in general, piezoelectric ceramics are more sensitive than thin polymer films. In piezoceramics, eigenmodes are excited by pressure pulses, leading to acoustic waves that decay exponentially within microseconds to milliseconds. Further pressure pulses reaching the detector within this time are overlaid by the signal from the first pulse. This is not observed when nanosecond pressure pulses are detected by thin piezoelectric polymer films. Therefore, ceramics are preferable for sensitive quantitative analyses in liquids, whereas piezoelectric polymer films are used, if the temporal pressure distribution is of importance, in pulsed PA depth profiling, for example.

In the analysis of liquid samples by pulsed PAS, in most cases the so-called forward mode is employed for signal detection. In this mode, excitation and detection are performed on different sides of the sample. Figure 5 shows the principal sensor arrangements for PA

measurements in weakly and strongly absorbing samples. The acoustic waveform generated depends on the shape of the acoustic source. In weak absorbers (Fig. 5a), attenuation of the laser beam inside the sample can be neglected. Thus, the laser builds a cylindrical acoustic source resulting in cylindrical waves, which can be detected perpendicularly to the laser beam (detector I). In opaque samples (Fig. 5b), low optical penetration depth leads to a punctiform acoustic source that generates spherical waves. Here, detection both along the laser beam (detector II) and perpendicular to it (detector I) is possible. In pulsed PA analysis of solid samples, the generated pressure pulses are often detected in backward mode, where excitation and detection are performed at the same side of the sample. Since piezoelectric transducers are generally not transparent, illumination through the piezo and detection at the same point are not possible. This can be overcome using the sensor set-ups shown in Fig. 6. The PA sensor in Fig. 6a uses a transparent prism as coupling material for both illumination of the sample and transfer of the acoustic energy to the detector. Another possibility is to illuminate the sample by means of an optical fiber and to detect the pressure pulses by a piezoelectric ring around the fiber (Fig. 6b).

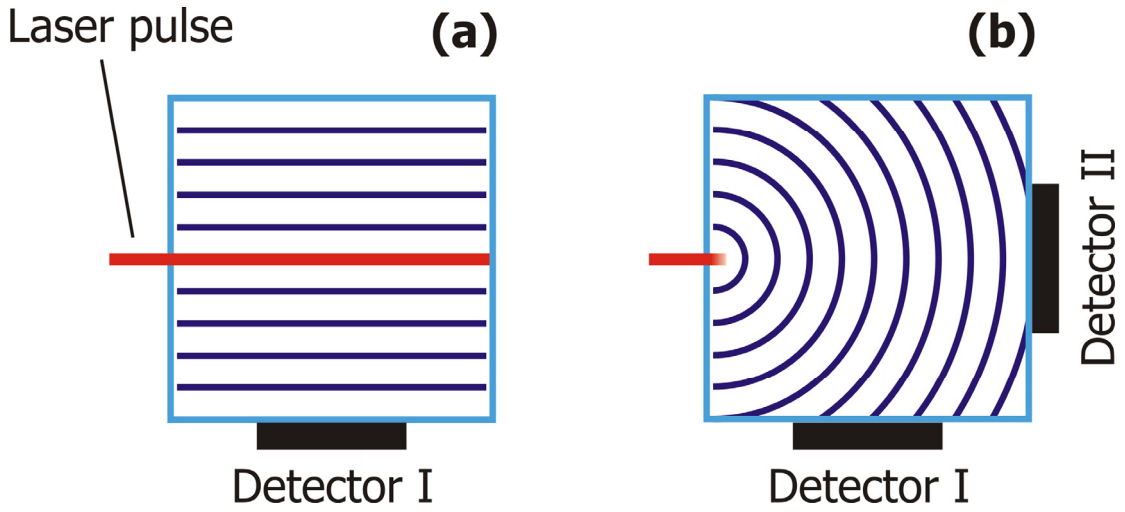


**Fig. 5a–b** Direct generation and forward mode detection of photoacoustic signals in weakly (**a**) and highly (**b**) absorbing samples.

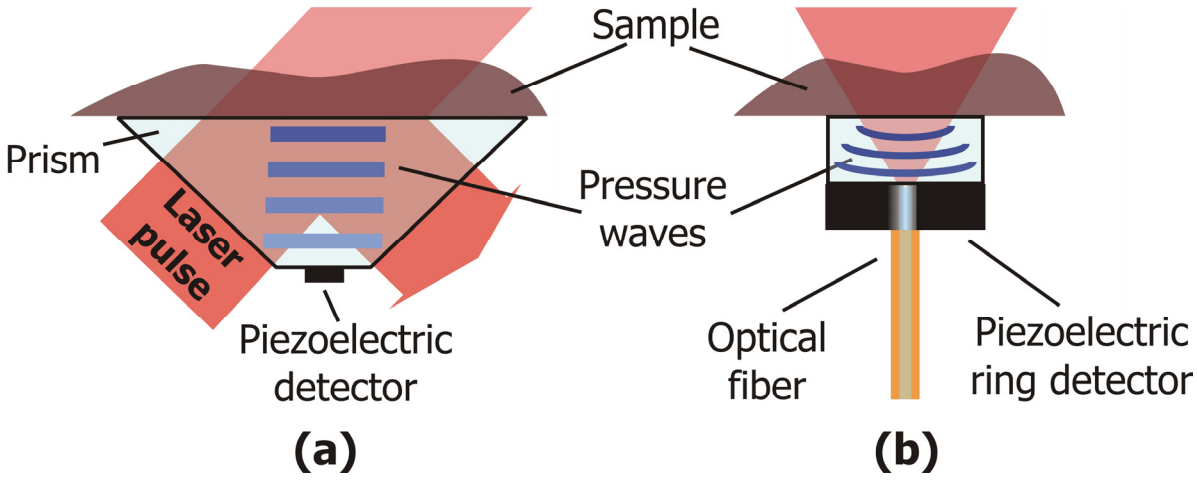


**Fig. 6a–b** Backward mode detection in solid samples: illumination through a transparent prism which also acts as acoustic coupling material (**a**) and detection by a piezoelectric ring (**b**).

In addition to conventional acoustic detection based on microphones or piezos, optical detection schemes for pressure waves are described in the literature. Optical microphones are applied in PA gas phase analysis [54, 55] and similar fiber optic sensors are reported for liquid phase analysis [56, 57]. Here, an optical fiber is wrapped onto a PA cell. Pressure changes inside the cell cause refractive index changes in the fiber which lead to phase shifts in the light coupled into the fiber and these can be detected, for example, by interferometry. In this case, the fiber is one arm of an interferometer. In PA investigations of condensed matter, optical methods can be employed for the detection of refractive index changes at an interface of the sample or measurement of the surface displacement caused by a pressure wave. In the first case, the sample is placed at the base of a transparent prism (see Fig. 7a). A continuous probe laser beam is reflected at the interface between prism and sample. A pressure wave transmitted through this interface will change the refractive index, resulting in variations of the optical reflectance, which can be detected optically. If a time-gated video camera is employed for detection, the pressure waves can be imaged in a two-dimensional and time-resolved fashion [58–60]. In the second case, the probe beam is one arm of an interferometer (see Fig. 7b). Pressure waves reaching the interface will cause surface displacements in the nanometer range, which can be detected due to changes in the interference pattern [62–65]. Such optical methods are advantageous due to their ability to perform non-contact measurements and their improved lateral resolution compared to piezoelectric detectors. For three-dimensional PA imaging, two-dimensional piezoelectric detector arrays have been proposed, but small piezosensors with fine spacing are hard to realize [66]. In optical detection, lateral resolution is only limited by the diameter of the probe beam, which can be less than 1 μm [58].

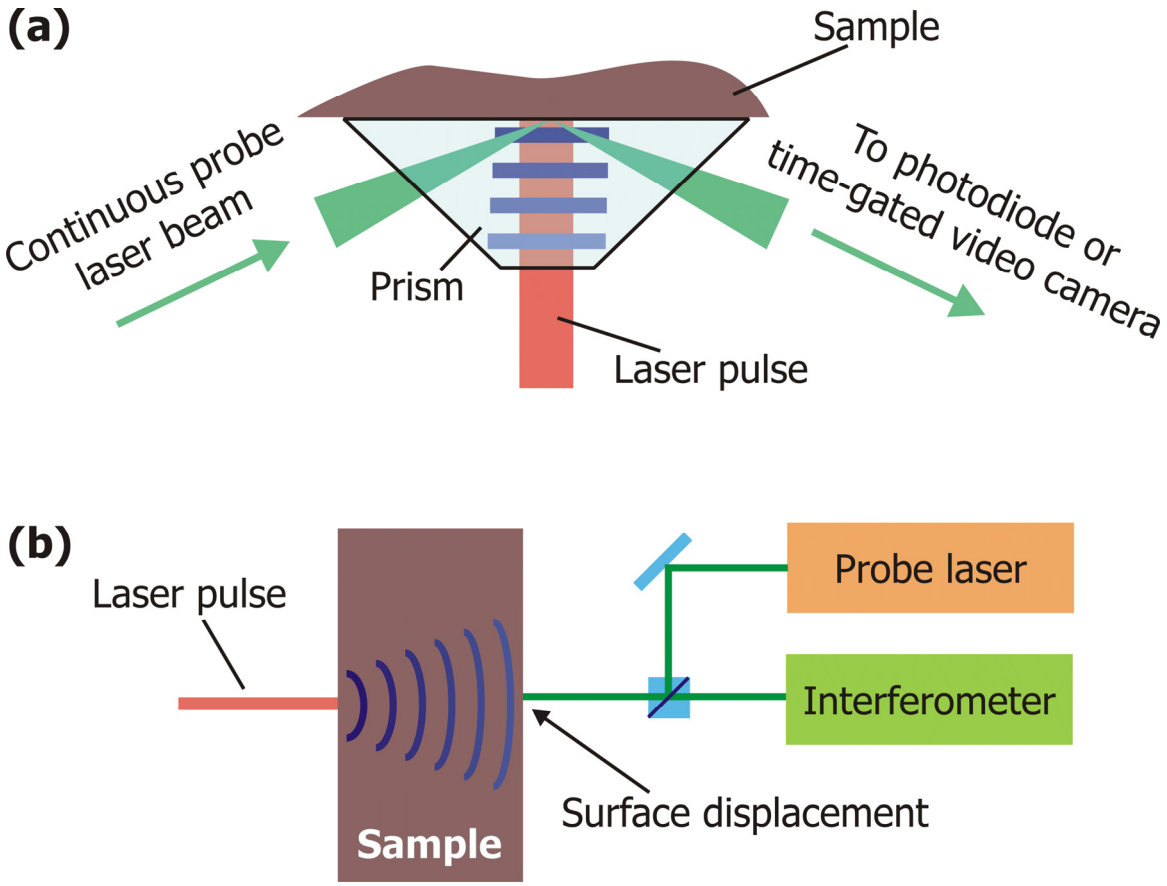


**Fig. 7a–b** Optical detection schemes in pulsed PAS: measurement of refractive index changes (**a**) and surface displacements (**b**).

Pressure waves generated in liquid and solid samples can be visualized directly by Schlieren photography or dark field imaging. These techniques allow the influence of optical properties and the illuminated volume fraction of the sample on the produced acoustic waveforms to be investigated [67, 68]. Since the sample needs to transmit light beams in order to be able to visualize the pressure waves, these techniques are restricted to transparent and non-scattering samples. To overcome this limitation, an interesting set-up was proposed: an acoustic lens system was used to image the initial transient pressure distribution inside the sample into a water container, where the three-dimensional pressure distribution could be detected by dark field imaging. In this way, absorbing objects inside a scattering matrix could be visualized as stereo images [69].

# 4 Applications of PAS in process analytical chemistry

## 4.1 Gas phase analysis

In recent years, the development of new PA set-ups for on-line gas monitoring has been achieved through new developments in diode lasers [70]. Until recently, chopped or modulated CO and $CO_2$ lasers were the most common powerful and tunable radiation sources for gas phase analysis in the mid-infrared range [71–73]. However, in the few last years, tunable and/or intense diode lasers became available, which allowed the development of sensitive, miniaturized and robust PA set-ups. Examples of the application of these recent laser developments to PAS are: lead salt diode lasers [74, 75], quantum cascade lasers [76–79], distributed feedback diode lasers [80], and external cavity lasers. Additionally, non-linear optical devices – such as optical parametric oscillators (OPO) [81] and difference frequency generation (DFG) [82] – have been used to generate selected wavelengths in the IR range. Thus, compact laser sources are available for PA gas phase analysis with emission powers ranging from milliwatts to watts, and covering the wavelength range from 800 nm up to 16 μm [70]. PA sensors have been developed for a huge number of gases, which are relevant in industrial and environmental studies [83–90]. An overview on analytes, limits of detection and laser sources can be found in [17]. Sensitivity can be improved by using multipass and intracavity PA cells [86–91]. The influence of acoustic noise generated by the cell windows or the gas flow was reduced by the development of acoustic notch filters, open and differential cells [19, 23, 92, 93].

Industrial plants have shown increasing interest in obtaining modern instruments for on-line monitoring of gaseous pollutants over the last few years, for several reasons. The exhaust gases from industrial plants have to be controlled for the sake of environmental protection (for example, reducing greenhouse gases) and to limit man-made disasters. Additionally, the monitoring of gas compositions is necessary for workplace security at industrial plants as well as to improve production processes and waste gas treatment [94]. There are several groups of main priority atmospheric pollutants that can be detected by PA measurement techniques, such as sulfur oxides (such as $SO_2$), nitrogen oxides ($NO_x$), carbon oxides (CO and $CO_2$), hydrogen sulfide, ammonia, methane, and aerosol particles (such as soot).

Within these gaseous pollutants, ammonia is of special interest, because a large number of man-caused failures in chemical plants during recent years have been related to explosions and fires initiated by this flammable gas [94]. As well as the toxicity and flammability of the ammonia itself, $NH_3$ concentration is an important parameter that has to be monitored during the reduction of nitrogen oxides in waste gas treatment. Stack gas emissions from power plants contain huge amounts of nitrogen oxides and therefore contribute significantly to photochemical smog and ozone formation as well as to the acidification of the soil. In order to reduce the $NO_x$ content, ammonia is added to the exhaust gas. Reduction of $NO_x$ by ammonia takes place via a catalyst. For process optimization and control of the exhaust gas, the ammonia concentration has to be monitored on-line [95]. Ammonia is also of interest because it is one of the main basic atmospheric components [96]. Deep UV photolithography for the generation of semi-conductor structures with dimensions of less than 200 nm is based on a chemically amplified resist (CAR). In this system, irradiation with a deep UV laser ($\lambda = 193$, 157 and 130 nm for example) generates a small number of acid molecules that initiate a catalytic cascade and lead to a trans-formation of the irradiated area. Thus, even low

concentrations of basic impurities can inhibit the photochemical process and reduce the lithographic performance [95]. Ammonia concentrations, which have to be monitored in clean rooms, the environment and in production plants, can vary over a wide range. In semiconductor processing, a few ppb or even less of ammonia can affect the photolithographic process. Atmospheric concentrations range from a few ppb up to several 100 ppb in polluted areas. In production plants, ammonia concentrations can range from ppm levels up to hundreds of ppm during leaks [94]. In these cases, the wide dynamic range and the low detection limits achievable in PA gas phase analysis are both advantageous. In recent years, PA sensors that are highly sensitive to ammonia have been presented [95, 97]. The lowest detection limit reported for ammonia is 0.1 ppb, with a measurement range of 0.1 ppb up to 3 ppm. The measurement system (TGA300 series) uses a $CO_2$ laser for excitation and a resonant PA cell, which enables on-line measurements at relatively high flow rates of up to 5 L $min^{-1}$ and short response times. These TGA 300 sensors have been successfully applied to process monitoring in the semiconductor industry and to air quality monitoring. Figure 8 depicts the sensor set-up, the resonance profile of the PA cell, a calibration curve, and a typical daily variation in the ammonia concentration in a clean room [95].

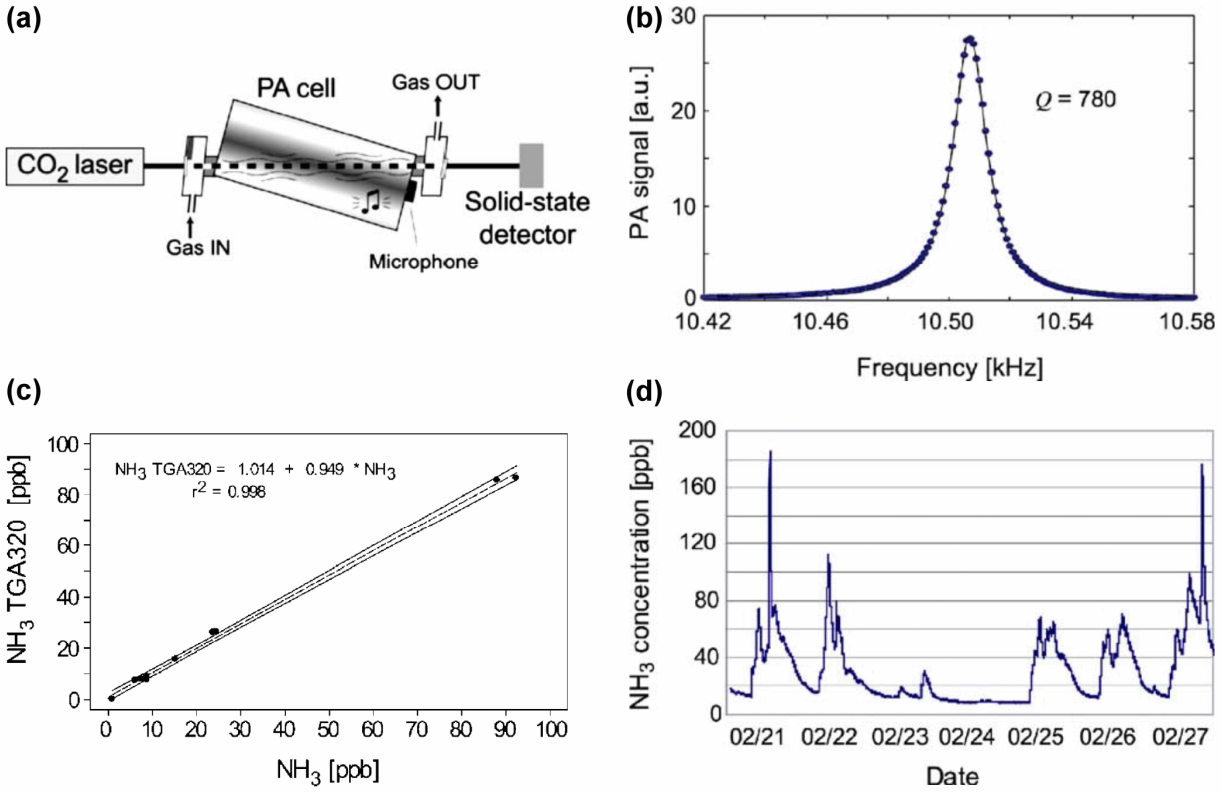


**Fig. 8a–d** Set-up for ammonia detection (**a**), resonance profile of the PA cell (**b**), calibration curve (**c**), and PA monitoring of the ammonia concentration in a clean room (**d**). The daily evolution shows the importance of contamination by staff activity: over the weekend (02/23 and 02/24) the concentration level drops, whereas it peaks in the mornings and afternoons of weekdays. Reprinted with permission from [95]. Copyright 2004 Elsevier.

Nitrogen dioxide is a component of automobile and industrial exhaust gases that plays an important role in ozone generation and the cycle of ozone in the troposphere. This compound has particular spectral features: absorption in the visible range and relative long excited level lifetimes. Thus, energy conversion into heat by collision is very effective. For excitation, robust and mobile Nd:YAG lasers with second harmonic generation are available which generate pulsed or

cw radiation at a wavelength of 532 nm. Using such laser sources, limits of detection of 20 and 15 ppb $NO_2$ could be achieved for modulated and pulsed excitation, respectively. In this way, $NO_2$ can be detected very selectively in the atmosphere, because other gaseous atmospheric components do not absorb green light [98].

New developments in diode lasers allowed the transfer of PAS to trace measurements of methane. Beside $CO_2$, methane is one of the main greenhouse gases and so has to be monitored in industrial exhaust gases. Excitation by low-power distributed feedback (DFB) diode lasers at 1.65 μm allows methane determination with a minimum detection limit of 6 ppm. Due to the direct proportionality between the PA signal and the incident radiation power, the detection limit will be lowered if laser diodes with a higher intensity at 1.65 μm become available [99]. Additional applications of PAS exist in the field of workplace security, in terms of monitoring of solvent vapors [100], as well as in fire detection and prevention via the measurement of combustable and flammable gases, respectively [101].

Exhaust gases from internal combustion engines also often have to be monitored, during attempts to improve the combustion process and when studying the exhaust gas treatment (by a catalyst, for instance). Therefore, PA sensors based on CO and $CO_2$ laser excitation have been developed for on-line monitoring of nitrous oxides, $CO_2$, water vapor and carbohydrates in the ppm range [102–104]. By using all 90 laser transitions accessible by CO laser excitation, it is possible to perform multicomponent analyses of exhaust gases from two-strike motorcycles, gasoline and diesel engines. The PA system allows ten compounds to be distinguished, even discriminating between the isomers of xylene [105]. In recent years, interest in the soot contents of vehicle exhausts has increased due to upcoming regulations encouraging the reduction of particulate emissions. These regulations require not only further improvements in combustion engines and exhaust gas treatment but also a new generation of real-time soot analyzers. A PA soot sensor (PASS, see Fig. 9a) allows the on-line measurement of diesel soot with a detection limit of 2 g $m^{-3}$ of black carbon, a linear range from 2 to 1200 g $m^{-3}$, and a temporal response of approximately 1 s. A high-power laser diode with $\lambda$ = 809 nm was employed for excitation. The NIR radiation at this wavelength is not absorbed by gaseous exhaust gas components (such as $NO_2$), allowing the selective determination of soot particles [106]. This set-up was applied successfully at engine test benches (see Fig. 9b) [106] and during experiments into the improved soot deposition systems for the removal of particulate matter [107, 108].

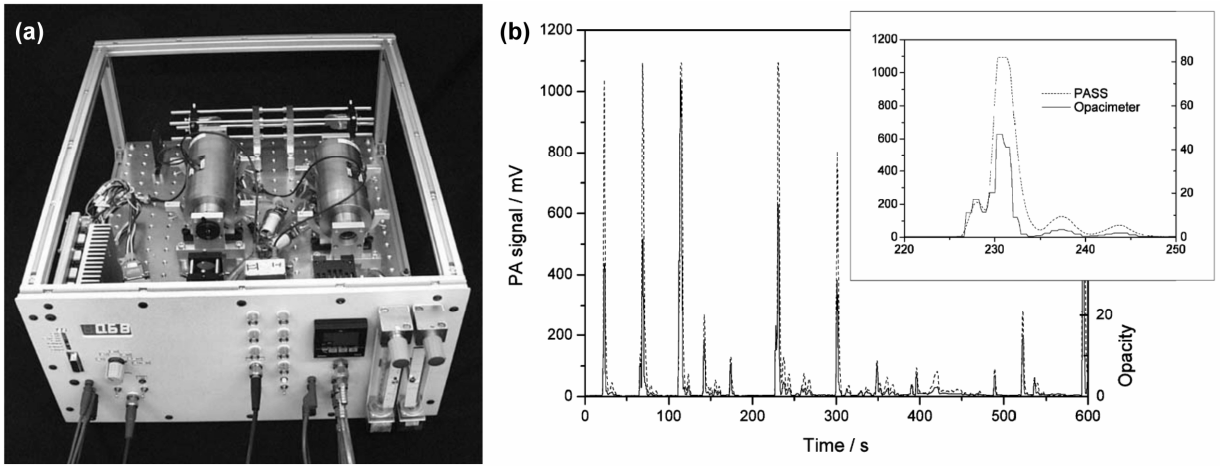


**Fig. 9a–b** Mobile photoacoustic soot sensor (*PASS*) in a 19 instrument rack (**a**) and European transient test cycle (*ETC*) monitored by PAS and opacimetry at a diesel engine test bench (**b**). Reprinted from [106]. Copyright 2003 Springer-Verlag.

Beside the monitoring of workplaces and industrial and diesel exhaust, PA gas phase analysis is employed in the optimization of postharvest processing and the storage of fruits. Here, the focus lies on ethylene measurements. This gaseous plant hormone is involved in the regulation of many physiological processes, like growth, maturation, and ripening, and is an important parameter governing the shelf-lives of fruits. Therefore, PA setups for ethylene monitoring in the ppb-ppm range have been developed [109, 110]. Systems for multicomponent measurements of various relevant analytes, such as ethylene, ammonia, ozone, and alcohols have also been described [111]. Sub-ppb detection limits for ethylene and other gaseous compounds were achieved with a multipass PA cell [112]. In other agricultural applications, PAS is used to monitor emission gases from extensively-managed grassland and fields [113, 114], seeds [115], and animal husbandry [116–118]. In the areas of food quality and food packaging, humidity is of paramount importance. PA water vapor sensors have detection limits in the sub-ppm range and dynamic ranges of more than four orders of magnitude [119].

In the context of PA gas phase analysis, the possibility of "indirect" sampling of condensed matter should also be mentioned. In this case, analytes are transferred from liquid or solid samples to the gas phase by chemical reactions or thermodesorption and detected by a PA gas analyzer. In this way, both the high sensitivity and the wide dynamic range available from gas phase PAS can be used on liquid and solid samples. Additionally, the selectivity of the measurements can be improved by selective analyte transfer into the gas phase. A method for determining the total inorganic carbonate (TIC) level is based on the generation of $CO_2$ by the reacting carbonate with perchloric acid. Using PA $CO_2$ detection in the gas phase, TIC contents ranging from 3 mol $L^{-1}$ to 36.4 mmol $L^{-1}$ $NaHCO_3$ in water and from 0.02 to 120 mg $CaCO_3$ in solids were automatically determined [120]. A set-up based on the thermodesorption of analytes from solid samples and subsequent PA detection in the gas phase was employed for the measurement of pentachlorophenol (PCP) in wood (see Fig. 10a). The fungicide PCP has been used for wood preservation since the 1950s. Although this compound has been restricted or banned in most of industrial countries since the 1980s due to the risks to human health, there are still problems due to the large amount of PCP-contaminated waste wood. Thermodesorption and subsequent PAS analysis allows a cost-effective on-site screening of wood samples via non-destructive measurements without sample pre-treatment. PA measurements in the NIR range (7800-4000 $cm^{-1}$) are not influenced by the moisture of wood and a detection limit of 10 g PCP/$cm^2$ surface area was achieved (see Fig.10b) [121].

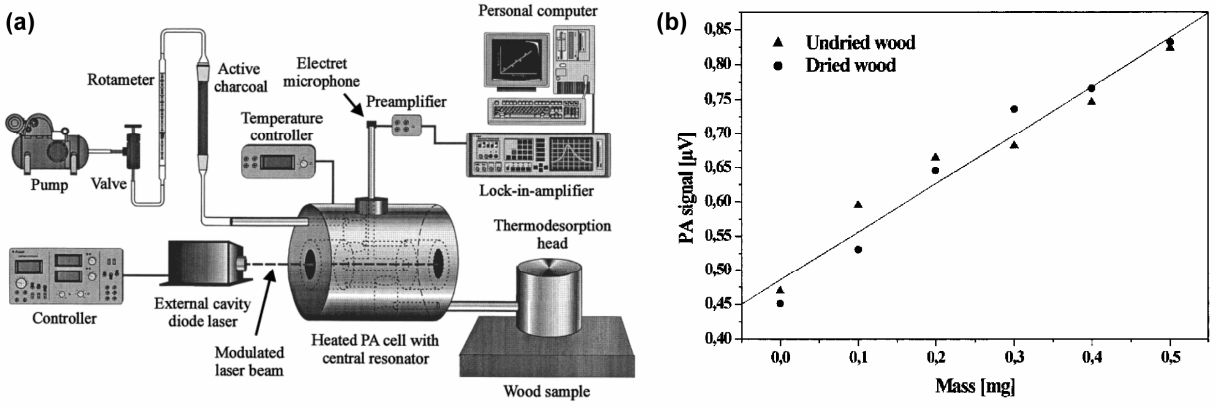


**Fig. 10a–b** Indirect sampling of wood and subsequent PA detection of pentachlorophenol (PCP) in the gas phase: set-up with thermodesorption head containing a halogen lamp (**a**) and calibration based on undried and dried wood samples (**b**). Reprinted with permission from [121]. Copyright 2000 American Chemical Society.

## 4.2 Indirect PA generation in condensed matter

In the indirect generation of PA signals in liquid and solid samples, commercially-available spectrometers coupled to a PA cell are usually employed for excitation, allowing the determination of UV/Vis and IR absorption spectra of opaque solids. The main application of UV/Vis–PAS is the characterization of semiconducting materials. Since PAS allows absorption spectra to be determined for solid samples, band gaps can be calculated directly from absorption edges in the spectra [122–124]. As the PA signal depends on heat diffusion, the thermal diffusivity can also be determined, which is strongly sensitive to the structural quality of the semiconducting material [125]. UV/Vis–PAS has also been employed to investigate the optical properties of synthetic mineral pigments [126] and the chemical bonding of Cu and Fe incorporated into sol gel glasses [127]. Furthermore, packaging materials have been characterized by PA measurements in the UV/Vis range. Using depth-resolved PAS, it was possible to estimate the thicknesses and moisture contents of varnish layers on base paper [128].

Indirect IR-PAS and FT-IR-PAS techniques have been mainly applied in the field of polymer research [129]. Here, IR absorption spectra, depth profiles, and thermal diffusivity and effusivity parameters [130, 131] are determined by PAS in order to characterize synthetic polymers and to improve the polymerization process. Polymers are often very difficult samples to characterize by conventional IR spectroscopy, because they can be found as pellets, chips, films, membranes as well as manufactured products. PAS measurements of polymers result in intense IR spectra with little or no sample preparation, even if the samples are polymer chips [132] or porous membranes [133]. PA measurements were successfully used to monitor copolymer formation. In this way, it was possible to investigate the influence of reactant pretreatment on cross-linking. Depth profiles elucidated the distributions of OH and $CH_2$ groups inside the polymerization product [134]. In the analysis of micrometer-thick polymer laminates and plasma polymer films, the PA technique allowed selective probing of the surface layer and bulk material [135, 136]. Figure 11a depicts photoacoustic IR spectra of polyethylene with and without a near-surface additive. To perform depth-resolved investigation of the samples, photoacoustic measurements were carried out at different modulation frequencies. By calculating the influence of the modulation frequency on the signal amplitude, the 100 Hz spectrum was converted to 5 kHz. In the homogeneous sample without additive, the converted spectrum matches the 5 kHz spectrum, whereas an inhomogeneous distribution of the additive led to differences in the corresponding spectra [137]. Depth-resolved PA measurements were also employed to investigate the effects of such polymer additives. Depth profiles of a hydroxyl band allowed weathered and unweathered polyethylene samples containing different amounts of an ultraviolet-protection additive to be distinguished (see Fig. 11b) [137].

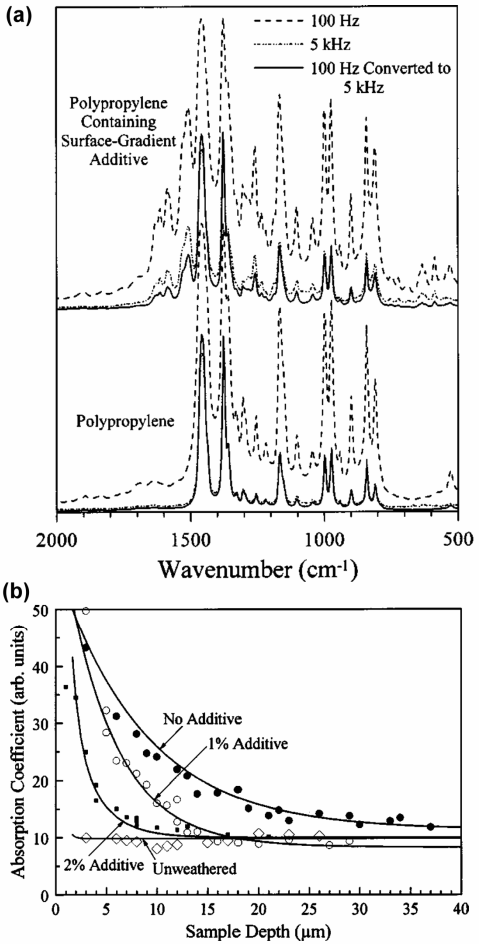


**Fig. 11a–b** PA spectra of polyethylene with and without a near-surface additive (**a**) and depth profiles of a hydroxyl band in weathered and unweathered PET containing different amounts of a UV-protection additive (**b**). Reprinted with permission from [137]. Copyright 2003 American Institute of Physics.

Depth profiling of the chemical composition of paper and paper coatings is essential when tailoring paper quality to the demands of recycling and new printing technologies. As mentioned above for UV/Vis-PAS, PA depth profiling was also applied to paper characterization in the infrared region. Biodegradable paper coatings consisting of cationized starch and the anionic surfactant sodium oleate were investigated, and studies revealed that the surfactant is enriched in the surface layer of the 20-60 μm-thick coating. This application demonstrated the potential of PAS in the development of new paper coatings [138].

FT-IR-PAS was also applied in the characterization of fossil fuels, where solid and liquid samples have been investigated. During the weathering of coking coal, a decrease in aliphatic hydrogen content was observed by evaluating FT-IR-PAS spectra. At the same time, shortening of hydrocarbon chains resulted in an increase of methyl with respect to methylene groups [139]. The FT-IR–PAS spectra obtained from different hydrocarbon distillation fractions provide useful information about the aliphatic hydrocarbon chains present in the samples [140]. Here, the abundance of $CH_2$ groups increases with increasing boiling point, whereas a decrease of $CH_3$-related signal intensities was observed in the same direction [141].

## 4.3 Direct PA generation in condensed matter

Pulsed PAS with direct generation is the PA technique most commonly used for the analysis of liquid samples. As in other PAS variants, the signal amplitude depends linearly on the absorption coefficient of the sample. However, generation of a PA pressure pulse in condensed matter also depends on the thermal expansion coefficient, the speed of sound, and the heat capacity of the sample matrix (see Eq. 5). In practice, absorption coefficients of liquids are usually determined after the sensor has been calibrated using well-defined samples or conventional absorption spectroscopy as a reference. Time-resolved analysis of PA signals offers the potential to perform calibration-less determination of absorption coefficients. If PA signals are generated by a collimated laser pulse and detected in forward mode (see Fig. 5, detector II), the rising edge of a time-resolved recorded signal represents the depth profile of the light distribution inside the sample [26]. In the case of a non-scattering absorber, exponential functions of the form $\exp(\mu_a c t)$ can be fitted to this part of the signal, with $c$ and $t$ denoting the speed of sound and the time, respectively. Similar signal shapes are obtained in samples that absorb and scatter light, allowing the determination of effective attenuation coefficients that describe the intensities of both absorption and scattering. The speed of sound, which must be known for data evaluation, can be determined by extracting the time delay between the laser pulse and pressure detection from the PA signal profile [142]. Thus, this form of PAS is a completely calibrationless technique for the determination of absorption coefficients, which can be applied to both dissolved and dispersed particulate analytes. This was successfully demonstrated by analyzing glucose solutions and graphite suspensions [143].

In both cases, calibrated sensors and calibrationless absorbance measurements, the main advantages of using PA to investigate liquids are the wide dynamic range (a few orders of magnitude), less influence from light scattering compared to conventional absorption spectroscopy, and the ability to analyze even highly absorbing and opaque samples without dilution [144]. Additionally, favorable combinations of thermal expansion coefficient, speed of sound, and heat capacity (see Eq. 5) in certain analytes or solvents lead to signal enhancement [145]. These features advantageously used in the analysis of hydrocarbon contamination in water. PA sensors based on pulsed excitation and piezoelectric detection allowed the determination of crude oil contamination in seawater with detection limits in the lower ppm range. The linear range of the measurement technique covered oil concentrations ranging from ppm to percent. Oil contents of even more than 20% could be determined with non-linear calibration functions, resulting in a dynamic range of approximately five orders of magnitude [146, 147]. Using Raman scattering in an optical fiber as a near-infrared source for pulsed PAS, it was possible to determine NIR spectra from hydrocarbons in water, even in regions characterized by strong absorption bands from water and thus, high opacity. These spectra permit us to choose laser diodes appropriate to this spectral range for further practical applications [148].

Another application, which covers a wide concentration range and both opaque and

scattering samples, is online process control in textile dyeing baths. For both dyeing process optimization and control of the wastewater, dye concentrations from a few mg $L^{-1}$ up to several g $L^{-1}$ have to be monitored. The conventional technique used for colorimetry in textile testing laboratories is reflection spectroscopy. Since the reflectance decreases with increasing absorbance, this technique often yields barely interpretable results with dark and saturated colorations. Therefore, the application of pulsed PAS is advantageous due to its wide dynamic range. A PA cell with a piezoelectric ceramic detector placed perpendicularly to the laser beam (see Fig. 5, detector I) allowed the determination of azo dye concentrations from a few mg $L^{-1}$ up to approximately 1 g $L^{-1}$ based on non-linear calibration functions. This cell was connected to the bath circulation of a dyeing apparatus in the form of a bypass with a constant flow rate of 200 mL $min^{-1}$. In this way, the decrease in dye concentration during a hightemperature dyeing process could be monitored with a temporal resolution of a few seconds [149]. By using a tunable OPO system for excitation, it was possible to obtain absorption spectra from highly concentrated dye solutions that were in good agreement with UV/Vis reference spectra, and concentration measurements in dye mixtures [150]. Plotting PAS versus UV/Vis reference data resulted in a measurement range limited by saturation effects at a 10 $cm^{-1}$. Optimizing PA detection led to an expansion of the dynamic range towards higher absorbances. By changing from a perpendicular geometry to detection along the laser beam (see Fig. 5, detector II), and using a piezoelectric PVDF film instead of a ceramic, the linear range was expanded to a 100 $cm^{-1}$. Using a non-linear calibration function, absorption coefficients of up to 200 $cm^{-1}$ can be determined. When performing simulated dyeing processes in the laboratory to demonstrate the potential of PAS in this field of application, textile dye concentrations from approximately 50 mg $L^{-1}$ up to 40 g $L^{-1}$ could be determined online with temporal resolutions of a few seconds [151].

Pulsed PAS of solid samples is often applied to depth profiling of layered samples and two-dimensional or three-dimensional tomography. Biofilms are layered biological systems, which are relevant in both natural and technical environments. They consist of microorganisms that are embedded in a gel formed by biopolymers. Microbial aggregates are used in wastewater treatment plants for the removal of organic and inorganic pollutants. On the other hand, in many technical processes biofilm formation is connected to negative effects, which are summarized by the term biofouling . Biofouling can lead to increased frictional resistance in tubes and pressure differences in membrane processes or a decreased heat transfer efficiency in heat exchangers. Biofilms can also clog nozzles and valves and can provide a habitat for pathogenic microorganisms. To optimize wastewater treatment plant processes and enhance biocide efficacy, a non-destructive technique for on-line monitoring of biofilms is needed. A PA technique based on backward mode piezoelectric detection (see Fig. 6a) allows the monitoring of biofilms formed on the base area of a sensor prism. Here, the signal amplitude increases with the biofilm's (optical) density, whereas depth-dependent features such as the biofilm thickness can be derived from the shapes of the PA signals. In this way, the influence of various process parameters (such as pH, flow conditions) on the structure and stability of the biofilm can be investigated [152]. Depth-resolved measurements with a resolution of ~ 10 μm allow the distributions of adsorbed particles [153] and detachment mechanisms [154] to be elucidated. The PA technique was applied successfully in order to compare the efficiencies of various biocides employed in printing technology to prevent biofouling. Strategies based on hydrogen peroxide, which were highly effective, led to a sloughing-off of relatively large biofilm areas. The photoacoustic depth profiles in Fig. 12 reflect the detachment of biomass and its transport from the substratum ($z = 0$ μm) towards the bulk liquid [154].

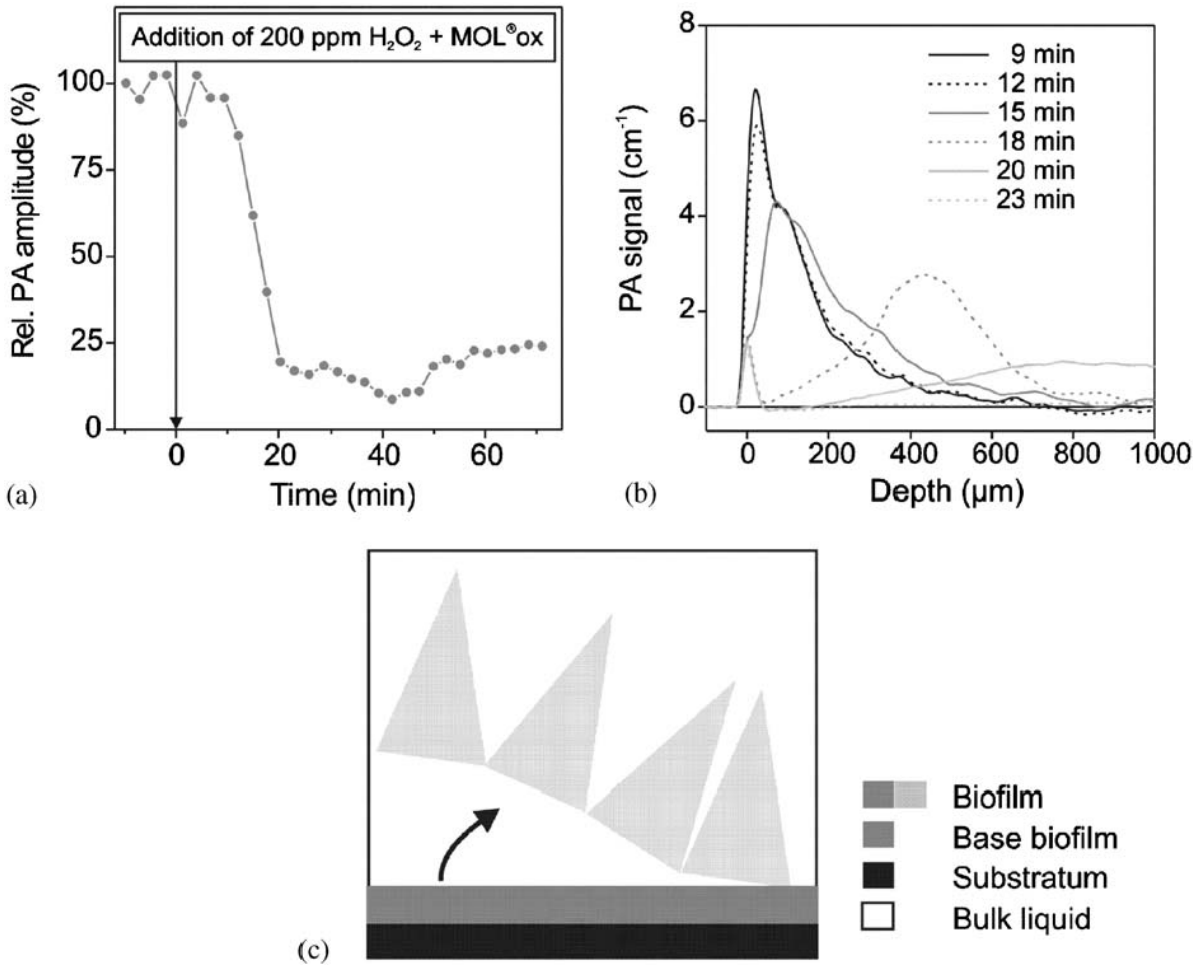


**Fig. 12a–c** PA monitoring of biofilm detachment caused by 200 mg L-1 hydrogen peroxide and the catalyst MOLox: PA signal amplitudes (**a**), depth profiles of the biomass (**b**), and sloughing-off mechanism derived from the depth profiles (**c**). Reprinted with permission from [154]. Copyright 2004 Elsevier.

The development of optical detection methods for pulsed PAS made non-contact measurements possible. This opened the door to a wide range of industrial applications allowing on-line measurements at conveyor belts and the characterization of materials with poor acoustic contact with piezosensors. For example, different paper materials could be characterized using interferometric detection. The study revealed the potential of this technique in the field of mechanical characterization of paper samples in the laboratory and on-line, on a paper machine. Piezoelectric detection would not be feasible in this case due to the damage caused to the paper samples by the contact transducers [155]. Aside from determination of mechanical properties, interferometric detection is also applied to depth profiling, allowing the measurement of painting thicknesses [156]. Other optical detection methods were applied to non-contact determinations of viscoelastic properties, thermal diffusivity, and thicknesses of thin films [157].

# 5 Conclusions

Photoacoustic spectroscopy (PAS) is based on optical absorption and subsequent detection of pressure fluctuations. The main advantages of this technique over conventional absorption spectroscopy are:

- Wide dynamic range (several orders of magnitude)
- Highly sensitive trace gas analysis with short pathlengths
- Measurement of high absorption coefficients, even in opaque samples, without sample dilution
- Determination of absorption spectra of solid samples, even in the form of powder, chips, or large objects
- Less influence from light scattering compared to conventional measurement techniques
- Depth profiling of layered samples

These features, allowing on-line measurements without sample pretreatment, are advantageous in process analysis. In the characterization of industrial products, additional benefits include the potential to determine absorption spectra of opaque solids and depth profiles of layered materials. For the analysis of gaseous, liquid, and solid samples, different combinations of excitation, signal generation and detection schemes have been developed. The most common PA techniques described in this article are:

1. Modulated excitation and direct generation of sound waves in gaseous samples
2. Modulated excitation of liquid and solid samples with subsequent indirect generation of sound waves in the adjacent gas phase
3. Pulsed excitation and direct generation of pressure pulses in liquid and solid samples

Methods (1) and (2), based on modulated excitation and detection of sound waves by microphones, are derived directly from A.G. Bell's photoacoustic experiments in 1880. The first analytical applications of PAS in the 1960s also used this principle. Today, commercial gas cells and UV/Vis and IR spectrometers are available that are based on these old PAS methods (examples can be found in [158–160]). The main application of gas phase PAS to process analytical technology is in the monitoring of workplaces and industrial and diesel exhaust in order to optimize waste gas treatment, combustion and production processes. Indirect PA generation in solid and liquid samples is employed to characterize semiconductors, synthetic polymers, paper coatings, and fossil fuels.

In recent years, PAS method (3), based on pulsed excitation and detection of pressure pulses, has been achieved through the development of new laser sources (such as tunable OPO systems) and detection methods (such as optical and interferometric detection). This technique is employed to investigate liquid samples, mainly due to its ability to determine absorption coefficients over a wide dynamic range, even in strongly absorbing and scattering samples. Sample pretreatment is not necessary in most cases. The need for calibration can also be overcome by extracting absorption coefficients directly from the signal shape. Applications related to technical processes include the detection of hydrocarbon contamination in water and the on-line monitoring of textile dyeing processes. Pulsed excitation in solid samples is used for both absorption measurements and depth profiling. Examples of the application of this include biofilm monitoring, measurement of painting thicknesses, and characterization of thin films and papers.

As we have seen, PAS has been applied in many fields of process analysis and the characterization of industrial materials. PAS techniques based on modulated excitation have been used in analytical chemistry since the 1960s, and measurement systems are already available commercially. Recent developments in pulsed PAS – especially in piezoelectric and optical detection – open up new avenues of application in two-dimensional and three-dimensional tomography and contactless on-line measurements.

# 6 References


1. Bell AG (1880) Am J Sci 305–324
2. Bell AG (1881) Phil Mag J Sci 11:510–528
3. Tyndall J (1881) Proc R Soc 31:307–317
4. Röntgen WC (1881) Ann Phys Chem 1:155–159
5. Viegerow ML (1938) Dokl Akad Nauk SSSR 19:687–688
6. Luft KF (1943) Z Tech Phys 5:97–104
7. Kerr EL, Atwood JG (1968) Appl Opt 7:915–921
8. Kreuzer LB (1971) J Appl Phys 42:2934–2943
9. Patel CKN, Burkhardt EG, Lambert CA (1974) Science 184:1173–1176
10. Rosencwaig A, Gersho A (1976) J Appl Phys 47:64–69
11. Patel CKN, Tam AC (1981) Rev Mod Phys 53:517–550
12. Kinney JB, Staley RH (1982) Ann Rev Mater Sci 12:295–321
13. Tam AC (1986) Rev Mod Phys 58:381–431
14. Rosencwaig A (1980) Photoacoustics and photoacoustic spectroscopy. Wiley, New York
15. McDonald FA, Wetsel GC (1978) J Appl Phys 49:2313–2322
16. McDonald FA (1981) J Appl Phys 52:1462–1463
17. Harren FJM, Cotti G, Oomens J, te Lintel Hekkert S (2000) In: Meyers RA (ed) Encyclopedia of analytical chemistry. Wiley, Chichester, pp 2203–2226
18. Sigrist MW (1994) In: Sigrist MW (ed) Air monitoring by spectroscopic techniques. Wiley, New York, pp 163–238
19. Miklós A, Hess P (2000) Anal Chem 72:30A–37A
20. Dewey CF, Kamm RD, Hackett CE (1973) Appl Phys Lett 23:633–635
21. Kamm RD (1976) J Appl Phys 47:3550
22. Karbach A, Hess P (1985) J Chem Phys 83:1075–1084
23. Miklós A, Hess P, Bozoki Z (2001) Rev Sci Instrum 72:1937–1955
24. Schäfer S, Miklós A, Pusel A, Hess P (1998) Chem Phys Lett 285:235–239
25. Gusev VE, Karabutov AA (1993) Laser optoacoustics. AIP, New York
26. Karabutov AA, Podymova NB, Letokhov VS (1995) J Mod Opt 42:7–11
27. Karabutov AA, Podymova NB, Lethokov VS (1995) Appl Opt 34:1484–1487
28. Karabutov AA, Podymova NB, Letokhov VS (1996) Appl Phys B 63:545–563
29. Burns DH (1994) Appl Spectrosc 48:12A–19A
30. Coufal H (1995) J Mol Struct 347:285–292
31. Karabutov AA, Savateeva EV, Podymova NB, Oraevsky AA (2000) J Appl Opt 87:2003–2014
32. Lohmann S, Ruff C, Schmitz C, Lubatschowski H, Ertmer W (1997) Lasers Med Sci 12:357–363
33. Oraevsky AA, Jacques SL, Tittel FK (1997) Appl Opt 36:402–415
34. Kopp C, Niessner R (1999) Appl Phys B 68:719–725
35. Beenen A, Spanner G, Niessner R (1997) Appl Spectrosc 51:51–57
36. Spicer JB, Wallace SL (1998) J Mater Sci 33:3899–3906
37. Vollmann J, Profunser DM, Dual J (2003) Rev Sci Instrum 74:851–853
38. Scruby CB, Smith RL, Moss BC (1986) NDT Int 19:307–131

39. Oberheide U, Christoph L, Krebs R, Welling H, Ertmer W, Lubatschowsky H (2002) Proc SPIE 4618:99–105

40. Oraevsky AA, Karabutov AA, Solomatin SV, Savateeva EV, Andreev VG, Gatalica Z, Singh H, Fleming RD (2001) SPIE 4256:6–15

41. Oraevsky AA, Savateeva EV, Solomatin SV, Karabutov AA, Andreev VG, Gatalica Z, Khamapirad T, Henrichs PM (2002) SPIE 4618:81–94

42. Reyman AM, Yakovlev IV, Kirillov AG, Lozhkarev VV (2001) Proc SPIE 4256:159–166

43. Selb J, Lévêque-Fort S, Pottier L, Boccara C (2001) Proc SPIE 4256:200–207

44. Wang X, Xu Y, Xu M, Yokoo S, Fry E, Wang LV (2002) Med Phys 29:2799–2805

45. McClelland JF, Jones RW, Bajic SJ (2002) In: Chalmers JN, Griffiths PR (eds) Handbook of vibrational spectroscopy. Wiley, New York

46. Dittmar RM, Chao JL, Palmer RA (1991) Appl Spectrosc 45:1104–1110

47. Michaelian KH (1989) Appl Spectrosc 43:185–190

48. Wang H, Phifer EB, Palmer RA (1998) Fresen J Anal Chem 362:34–40

49. Jackson W, Amer NM (1980) J Appl Phys 51:3343–3353

50. Nelson ET, Patel CKN (1981) Opt Lett 6:354–356

51. Wu L, Wei CC, Wu TS, Liu HC (1983) J Phys C 16:2813–2821

52. Ogi H, Kawasaki Y, Hirao M, Ledbetter H (2002) J Appl Phys 92:2451–2456

53. Sessler GM (1981) J Acoust Soc Am 70:1596–1608

54. Bilaniuk N (1997) Appl Acoust 50:35–63

55. Breguet J, Pellaux JP, Gisin N (1995) Sensor Actuat A 48:29–35

56. Kawabata Y, Yasunaga K, Imasaka T, Ishibashi N (1993) Anal Chem 65:3493–3496

57. Hand DP, Hodgson P, Carolan TA, Quan KM, Mackenzie HA, Jones JDC (1993) Opt Commun 104:1–6

58. Paltauf G, Schmidt-Kloiber H, Köstli KP, Frenz M (1999) Appl Phys Lett 75:1048–1050

59. Köstli KP, Frenz M, Weber HP, Paltauf G, Schmidt-Kloiber H (2000) J Appl Phys 88:1632–1637

60. Paltauf G, Schmidt-Kloiber H (2000) J Appl Phys 88(3):1624–1631

61. Dewhurst RJ, Shan Q (1999) Meas Sci Technol 10:R139–R168

62. Park SM, Diebold DJ (1987) Rev Sci Instrum 58:772–775

63. Chu JH, Bak YH, Kang BK, Kim U, Oum KW, Choi JG, Ko DS (1992) Opt Commun 89:135–139

64. Carp SA, Guerra A, Duque SQ, Venugopalana V (2004) Appl Phys Lett 85:5772–5774

65. Payne BP, Venugopalan V, Mikic BB, Nishioka NS (2003) J Biomed Opt 8:273–280

66. Hoelen CGA, de Mul FFM, Pongers R, Dekker A (1998) Opt Lett 23:648–650

67. Emmony DC, Siegrist M, Kneubuehl FK (1976) Appl Phys Lett 9:547–549

68. Niederhauser JJ, Frauchiger D, Weber HP, Frenz M (2002) Appl Phys Lett 81:571–573

69. Niederhauser JJ, Jaeger M, Frenz M (2004) Appl Phys Lett 85:846–848

70. Sigrist MW (2003) Rev Sci Instrum 74:486–490

71. Urban W (1995) Infrared Phys Technol 36:465–473

72. Bijnen FGC, Harren FJM, Hackstein JHP, Reuss J (1996) Appl Opt 35:5357–5368

73. Witteman WJ (1987) Springer Ser Opt Sci 53

74. Kania P, Civi S (2003) Spectrochim Acta A 59:3063–3074

75. Werle P, Slemr F, Maurer K, Kormann R, Mücke R, Jänker B (2002) Opt Lasers Eng 37:101–114

76. Faist J, Capasso F, Sivco DL, Sirtori C, Hutchinson AL, Cho AY (1994) Science 264:553

77. Beck M, Hofstetter D, Aellen T, Faist J, Oesterle U, Ilegems M, Gini E, Melchior H (2002) Science

295:301–305

78. Nägele M, Hofstetter D, Faist J, Sigrist MW (2001) Anal Sci 17:s497–s499

79. Barbieri S, Pellaux JP, Studemann E, Rosset D (2002) Rev Sci Instrum 73:2458–2461

80. Schäfer S, Mashni M, Sneider J, Miklós A, Hess P, H Pitz H, Pleban KU, Ebert V (1998) Appl Phys B 66:511–516

81. Baxter GW, Paine MA, Austin BDW, Halloway CA, Haub JG, He Y, Milce AP, Nibler JF, Orr BJ (2000) Appl Phys B 71:651–663

82. Byer RL, Herbst RL (1977) Top Appl Phys 16:81–137

83. West GA (1983) Rev Sci Instrum 54:797–817

84. Loper GL, Sasaki GR, Stamps MA (1982) Appl Opt 21:1648–1653

85. Crane RA (1978) Appl Opt 17:2097–2102

86. Harren FJM, Bijnen FGC, Reuss J, Voesenek LACJ, Blom CWPM (1990) Appl Phys B 50:137–144

87. Harren FJM, Berkelmans R, Kuiper K, te Lintel Hekkert S, Scheepers P, Dekhuijzen R, Hollander P, Parker DH (1999) Appl Phys Lett 74:1761–1763

88. Koch KP, Lahmann W (1978) Appl Phys Lett 32:289–291

89. Fung KH, Lin HB (1986) Appl Opt 25:749–752

90. Naegele M, Sigrist MW (2000) Appl Phys B 70:895–901

91. Rey JM, Marinow D, Vogler DE, Sigrist MW (2005) Appl Phys B 80:261–266

92. Miklòs A, Lörincz A (1989) Appl Phys B 48:213–218

93. Zeninari V, Kapitanov VA, Courtois D, Ponomarev YN (1999) Infrared Phys Technol 40:1–23

94. Sazhin SG, Soborover EI, Tokarev SV (2003) Russ J Nondestruct 39:791–806

95. Schilt S, Thévenaz L, Niklés M, Emmenegger L, Hüglin C (2004) Spectrochim Acta A 60:3259–3268

96. Dean KR, Miller DA, Caprio RA, Petersen JS, Rich GK (1997) J Photopolym Sci Technol 10:425–444

97. Pushkarsky MB, Webber ME, Baghdassarian O, Narasimhan LR, Patel CKN (2002) Appl Phys B 75:391–396

98. Slezaka V, Santiagob G, Peuriot AL (2003) Opt Laser Eng 40:33–41

99. Schäfer S, Mashni M, Sneider J, Miklós A, Hess P, Pitz H, Pleban KU, Ebert V (1998) Appl Phys B 66:511–516

100. Radak BB, Petkovska MT, Trtica MS, Miljanic SS, Petkovska LT (2004) Anal Chim Acta 505:67–71

101. Nebiker PW, Pleisch RE (2002) Fire Safety J 37:429–436

102. Bernegger S, Sigrist MW (1990) Infrared Phys 30:375–429

103. Schramm DU, Sthel MS, da Silva MG, Carneiro LO, Junior AJS, Souza AP, Vargas H (2003) Infrared Phys Technol 44:263–269

104. Schramm DU, Sthel MS, da Silva MG, Carneiro LO, Souza AP, Vargas H (2003) Rev Sci Instrum 74:513–515

105. Sigrist MW (1995) Infrared Phys Technol 36:415–425

106. Beck HA, Niessner R, Haisch C (2003) Anal Bioanal Chem 375:1136–1143

107. Messerer A, Rothe D, Pöschl U, Niessner R (2004) Top Catal 30/31:247–250

108. Rothe D, Zuther F, Jacob E, Messerer A, Pöschl U, Niessner R, Knab C, Mangold M (2004) SAE Technical Paper 2004-01-3046

109. da Silva MG, Lima JAP, Sthel MS, Marín E, Gatts CEN, Cardoso SL, Campostrini E, Pereira MG, Campos AC, Massunaga MSO, Vargas H (2001) Anal Sci 17:S534–S537

110. da Silva MG, Santos EO, Sthel MS, Cardoso SL, Cavalli A, Monteiro AR, de Oliveira JG, Pereira MG, Vargas H (2003) Rev Sci Instrum 74:703–705

111. Moeckli MA, Hilbes C, Sigrist MW (1998) Appl Phys B 67:449–458

112. Nägele M, Sigrist MW (2000) Appl Phys B 70:895–901

113. Tilsner J, Wrage N, Lauf J, Gebauer G (2003) Biogeochemistry 63:229–247

114. van Groenigen JW, Kasper GJ, Velthof GL, van den Pol-van Dasselaar A, Kuikman PJ (2004) Plant Soil 263:101–111

115. Bicanic D, Persijn S, Taylor A, Cozijnsen J, van Veldhuyzen B, Lenssen G, Wegh H (2003) Rev Sci Instrum 74:690–693

116. Williams JR, Chambers BJ, Hartley AR, Ellis S, Guise HJ (2000) Soil Use Manage 16:237–243

117. Monteny GJ, Groenestein CM, Hilhorst MA (2001) Nutr Cycl Agroecosys 60:123–132

118. Nicks B, Laitat M, Vanderheede M, Désiron A, Verhaeghe C, Canart B (2003) Anim Res 52:299–308

119. Bozóki Z, Szakáll M, Mohácsi A, Szabó G, Bor Z (2003) Sensor Actuat B 91:219–226

120. Liu W, Sun Z, Ranheimer M, Forsling W, Tang H (1999) Analyst 124:361–365

121. Beck HA, Bozóki Z, Niessner R (2000) Anal Chem 72:2171–2176

122. Kim HG, Kim WT (1990) Phys Rev B 8541–8544

123. Park S, Lee SK, Leet JY, Kim JE, Park HY, Park HL, Lim H, Kim WT (1992) J Phys Condens Matter 4:579–586

124. Pickett NL, Riddell FG, Foster DF, Cole-Hamilton DJ, Fryer JR (1997) J Matter Chem 7:1855–1866

125. Zakrzewski J, Firszt F, gowski S, M czy ska H, Marasek A, Pawlak M (2003) Rev Sci Instrum 74:572–574

126. Guskos N, Papadopoulos GJ, Likodimos V, Patapis S, Yarmis D, Przepiera A, Przepiera K, Majszcyk J, Typek J, Wabia M, Aidinis K, Drazek Z (2002) Mater Res Bull 37:1051–1061

127. Jáñes-Limón JM, Pérez-Robles JF, González-Hernández J, Vorobiev YV, Romano JA, Gandra FGC, da Silva EC (2000) J Sol-Gel Sci Techn 18:207–217

128. Walther HG, Christ A (2001) J Appl Phys 89:4124–4127

129. Schmatloch S, Schubert US (2004) Macromol Rapid Commun 25:69–76

130. Leite NF, Cella N, Vargas H, Mirando LCM (1987) J Appl Phys 61:3025–3027

131. Sanchez RR, Rieumont JB, Cardoso SL, da Silva MG, Sthel MS, Massunaga MSO, Gatts CN, Vargas H (1999) J Braz Chem Soc 10:97–103

132. Rintoul L, Panayiotou H, Kokot S, George G, Cash G, Frost R, Bui T, Fredericks P (1998) Analyst 123:571–577

133. Boccaccio T, Bottino A, Capannelli G, Piaggio P (2002) J Membr Sci 210:315–329

134. Dias DT, Medina AN, Basso ML, Bento AC, Porto MF, Rubira AF (2002) J Phys D Appl Phys 35:3240–3248

135. Dittmar RM, Chao JL, Palmer RA (1991) Appl Spectrosc 45:1104–1110

136. Jiang EY, Palmer RA, Barr NE, Morosoff N (1997) Appl Spectrosc 51:1238–1244

137. McClelland JF, Jones RW, Luo S (2003) Rev Sci Instrum 74:285–290

138. Halttunen M, Tenhunen J, Saarinen T, Stenius P (1999) Vibr Spectrosc 19:261–269

139. Cimadevilla JLG, lvarez R, Pis JJ (2003) Vibr Spectrosc 31:133–141

140. Michaelian KH (2003) Rev Sci Instrum 74:659–662

141. Michaelian KH, Hall RH, Bulmer JT (2003) Spectrochim Acta A 59:2971–2984

142. Shen Y, Spiers S, MacKenzie HA (2001) Anal Sci 17:S221–S222

143. Shen Y, Lu Z, Spiers S, MacKenzie HA, Ashton HS, Hannigan J, Freeborn SS, Lindberg J (2000) Appl Opt 39:4007–4012

144. Terzi M, Jovanovi -Kurepa J, Slivka J (1998) J Phys D Appl Phys 31:1368–1374

145. MacKenzie HA, Christison GB, Hodgson P, Blanc D (1993) Sensor Actuat B 11:213–220

146. Hodgson P, Quan KM, MacKenzie HA, Freeborn S, Hannigan J, Johnston EM, Greig F, Binnie TD (1995) Sensor Actuat B 29:339–344

147. Freeborn SS, Hannigan J, Greig F, Suttie RA, MacKenzie HA (1998) Rev Sci Instrum 69:3948–3952

148. Hannigan J, Greig F, Freeborn SS, MacKenzie HA (1999) Meas Sci Technol 10:93–99

149. Bahners T, Schlosser U, Schollmeyer E (1998) Sensors Update 4:141–166

150. Schlosser U, Schollmeyer E, Schmid T, Helmbrecht C, Haisch C, Niessner R (2003) Melliand Textilber 9:759–761

151. Schmid T, Helmbrecht C, Haisch C, Panne U, Niessner R (2003) Anal Bioanal Chem 375:1130–1135

152. Schmid T, Panne U, Haisch C, Hausner M, Niessner R (2002) Environ Sci Technol 36:4135–4141

153. Schmid T, Helmbrecht C, Panne U, Haisch C, Niessner R (2003) Anal Bioanal Chem 375:1124–1129

154. Schmid T, Panne U, Adams J, Niessner R (2004) Water Res 38:1189–1196

155. Lafond EF, Brodeur PH, Gerhardstein JP, Habeger CC, Telschow KL (2002) Ultrasonics 40:1019–1023

156. Drake TE (2003) International Patent WO 03/095942 A2

157. Rogers JA, Nelson KA (1996) Physica B 219/220:562–564

158. MTEC Photoacoustics Inc. (1998) Homepage. MTEC Photoacoustics Inc., Ames, IO. See http://www.mtecpas.com, accessed May 2005

159. Innova (2005) Homepage. Innova AirTech Instruments A/S, Ballerup, Denmark. See http://www.innova.dk, accessed May 2005

160. AVL (2005) Homepage. AVL List GmbH, Graz, Austria. See http://www.avl.com, accessed May 2005